ELSEVIER

Contents lists available at ScienceDirect

Journal of Solid State Chemistry

journal homepage: www.elsevier.com/locate/jssc



Low-temperature solvothermal fluorination method and synthesis of La₄Ni₃O₈F_x oxyfluorides via the La₄Ni₃O₈ infinite-layer intermediate



Colin K. Blakely ^a, Shaun R. Bruno ^a, Shannon K. Kraemer ^a, Artem M. Abakumov ^b, Viktor V. Poltavets ^c, *

- ^a Department of Chemistry, Michigan State University, East Lansing, MI, 48824, USA
- ^b Skolkovo Institute of Science and Technology, Moscow, Russia
- ^c Department of Chemistry and Advanced Materials Research Institute, University of New Orleans, New Orleans, LA, 70148, USA

ARTICLE INFO

Keywords: Solvothermal fluorination Oxyfluoride Low temperature fluorination Metastable

ABSTRACT

A novel facile solvothermal fluorination method was developed for metastable oxyfluorides preparation by filling anion vacancies in parent structures. High solubility of XeF_2 in acetonitrile and polarity of the solvent allowed for lower reaction temperature. The validity of the method was demonstrated by the preparation of a known oxyfluoride, $SrCoO_{2.5}F_{0.5}$, at unprecedented low temperature ($100\,^{\circ}C$). Additionally, two new oxyfluorides with idealized stoichiometry of $La_4Ni_3O_8F_1$ and $La_4Ni_3O_8F_2$, were prepared by the solvothermal fluorination via the $La_4Ni_3O_8$ infinite-layer intermediate. The proposed method allows preparation of metastable oxyfluorides, utilizes only inexpensive commercial autoclaves and can potentially find widespread utilization in materials synthesis.

1. Introduction

Low temperature fluorination of complex metal oxides allows for the syntheses of many metastable oxyfluorides [1-3], including high temperature superconductors [4,5], magnetic materials [6,7], and phases with unusual crystal structure motifs [8,9]. Many fluorination agents are utilized as alternatives to hazardous F2 gas [4,6], including polyvinylidene fluoride (PVDF) [9,10], MF₂ (M = Cu, Ni, Zn, Ag) [7,11], NH₄F [11] and XeF₂ [5,12,13]. However, PVDF requires temperatures above 150 °C, even for thin film fluorination [14]; MF₂ usage leads to the presence of metal oxide admixture in the final product and utilization of NH₄F often results in the formation of highly thermodynamically stable admixtures of alkaline earth fluorides or rare earth oxyfluorides [11]. In spite of the high vapour pressure of XeF2 of 0.5 atm at 100 °C [15], fluorination is severely kinetically hindered at this temperature, preventing the synthesis of well crystalline pure compounds [5]. However, fluorination technique efficient in the 50–150 °C temperature range can potentially provide access to many new metastable oxyfluorides by utilizing a chimie douce (soft chemistry) approach. Unlike conventional high-temperature reactions, which result in the preparation of thermodynamically stable products, the low-temperature soft chemistry approach allows for the formation of new metastable phases with unique structural features and/or unusual metal oxidation states. During soft chemistry transformations either a cationic or an anionic sublattice remains unchanged, i.e., such reactions are topochemical in nature. Recently, fluorination by XeF_2 under solvothermal conditions was utilized for a topotactic anion exchange in which $Gd_{1-x}Tb_xF_3$ fluorides were prepared from $Gd_{1-x}Tb_xOCl$ oxychlorides [16].

Mixed metal oxides with O vacancies are often employed as starting phases for oxidative fluorination. For example, the synthesis of SrCoO_{2.5}F_{0.5} was recently reported [6]. The phase was prepared by fluorination of the $Sr_2Co_2O_5$ brownmillerite by 10% $F_{2(g)}/90\%$ $N_{2(g)}$ at 220 °C [6]. The A₂B₂O₅ brownmillerite lattice is a derivative of the ABO₃ perovskite structure with ordered oxygen vacancies. As the result of the vacancies ordering, layers of alternating corner-sharing BO6 octahedra and BO₄ tetrahedra are present in the brownmillerite structure. Ordered oxygen vacancies can potentially serve as a template for synthesis of oxyfluorides with specific O/F ordering [12]. In brownmillerites, F diffusion by a vacancy mechanism involves O positions in layers adjacent to vacancies layers and lead to O/F mixing in the former tetrahedra layer. However, considering the lower activation energy for F⁻ diffusion than that for O²⁻ in oxides [17], it might hypothetically be possible to preserve BO₂ layers in BO₆ octahedra; thus, forming a ABO_{2.5}F_{0.5} perovskite structure with F-rich and F-free blocks. In order to increase the probability of anion ordering during synthesis, it is important to perform anion intercalation at as low a temperature as possible to avoid thermal

E-mail address: vpoltave@uno.edu (V.V. Poltavets).

 $^{^{\}ast}$ Corresponding author.

randomization of the anions. With this fact in mind, a new facile and active at low temperature fluorination method is needed.

Traditionally, reactions of oxides with XeF_2 are performed as solid-solid or solid-gas processes. At the same time, solvent addition was shown to be beneficial for a low temperature oxygen deintercalation process [18]. Stability [19,20] and high solubility [20] (32 g per 100 ml of solution at 21 °C) of XeF_2 in acetonitrile (CH₃CN) was reported. Among several studied solvents "inert" toward XeF_2 , CH₃CN was the only one with negligible side reactions [19]. Literature reports on solvothermal fluorination seems to be limited to fluorination of Sr_2CuO_3 and $NdSr_2Cu_2O_{6-\sigma}$ by NH_4HF_2 in absolute alcohol [21]. A SrF_2 admixture was observed in all fluorinated samples, as is common for this fluorination reagent [21].

In this communication, a new facile low temperature procedure of solvothermal fluorination by XeF_2 in CH_3CN is reported. The preparation of $SrCoO_{2.5}F_{0.5}$ at unprecedented low temperature (100 $^{\circ}C$) and synthesis of two new oxyfluorides, $La_4Ni_3O_8F_1$ and $La_4Ni_3O_8F_2$ are presented to demonstrate the validity of the new method.

2. Materials and methods

2.1. Synthesis of precursor oxides

Syntheses of the precursor oxide phases $Sr_2Co_2O_5$ and $La_4Ni_3O_8$ were performed according to previous reports [18,22,23]. Quenching from 1000 °C into liquid N_2 was required to avoid $Sr_2Co_2O_5$ brownmillerite conversion into the cubic O deficient perovskite upon cooling below 1000 °C. $La_4Ni_3O_8$ was prepared by the reduction of the $La_4Ni_3O_{10}$ powder in flowing pure hydrogen at 325 °C [23].

2.2. Solvothermal fluorination

All operations with XeF $_2$ and oxyfluorides were performed under inert atmosphere in a glovebox. At room temperature XeF $_2$ is a highly reactive solid (T_{melting} = 402.18 K [24]) and should be handled by Teflon or nickel spatulas. Utmost care should be taken to avoid exposing of XeF $_2$ to moisture, as hazardous HF will form. Exposure to HF in even minute quantities can lead to severe respiratory tract, eye, and skin burns. The solvothermal fluorination procedure was performed in commercial, Teflon-lined steel autoclaves (Parr Instrument 4744). For the fluorination, 200 mg of an oxide was suspended in a 1 M solution of XeF $_2$ in anhydrous CH $_3$ CN (5x molar excess XeF $_2$) in a 45 mL steel autoclave and sealed. The autoclaves were removed from the glovebox for a thermal treatment at appropriate temperatures (see below). After the reaction vessels cooled to room temperature, the black products were washed with anhydrous CH $_3$ CN several times under inert atmosphere.

2.3. Characterization methods

The samples were characterized by Powder X-ray diffraction (PXD) on a Bruker D8 Advanced diffractometer using Cu K α radiation. The patterns were recorded at room temperature with a step size of 0.02° (2 Θ). A dome-shaped air-free sample holder was used to measure the diffraction pattern of the moisture sensitive oxyfluorides. Rietveld refinement [25] of the obtained data was performed with GSAS [26] program with EXPGUI [27] interface.

The temperature dependence of DC magnetic susceptibility was measured on powder samples with a Quantum Design SQUID magnetometer at H=3000 Oe in the temperature range 4–300 K. Samples were loaded into gelatine capsules under N_2 , placed into a plastic sample holder and cooled to 4 K under zero magnetic field. The measurements were performed by warming the samples in the applied field after cooling to 4 K in zero field (ZFC, zero field cooling) and by cooling the samples in the applied measuring field (FC, field cooling).

3. Results and discussions

3.1. Solvothermal fluorination by XeF2 in acetonitrile

Approximately equal amounts of Sr₂Co₂O₅ and SrCoO_{2,5}F_{0,5} were observed by powder X-ray diffraction method (PXD) after the solvothermal fluorination was performed at 50 °C for 10 days. Increasing the reaction time at 50 °C had little effect on the final product composition, indicating that the reaction is severely kinetically hindered. After observing similar results at 75 $^{\circ}$ C, the reaction temperature was raised to 100 °C while keeping all other variables constant, which resulted in single phase SrCoO_{2.5}F_{0.5}. Rietveld refinement (Fig. 1, Table 1) in the $Pm\overline{3}m$ space group with a shared O/F position converged with $R_{wp} =$ 1.68%, $R_p = 1.58\%$, and $\chi^2 = 0.961$. The refined lattice parameter a =3.8549 (1) Å is in good agreement with the literature data [6]. Magnetic properties of the prepared sample indicated spin-canted antiferromagnetic transitions analogous to the literature data (Fig. 2). The increase of magnetic susceptibility at low temperatures is associated with a canted antiferromagnetism state. A bifurcation of the FC and ZFC magnetic susceptibility curves occurs at T ~30 K, similar to what was previously reported [6]. The inset displays M(H) measurement at 2 K, where a hysteresis is observed. The hysteresis behaviour only occurs below 30 K, found by measuring the M(H) curves at various temperatures.

An analogous solid-state reaction without CH₃CN was performed at 100 $^{\circ}$ C, resulting in a 0.45:0.55 mixture of Sr₂Co₂O₅: SrCoO_{2.5}F_{0.5}; therefore, fluorination with XeF₂ at solvothermal condition is more efficient than in the gaseous phase.

Several factors can lead to higher XeF2 activity under solvothermal conditions at low temperatures. The high solubility of XeF2 in CH3CN allowed the use of a 1 M solution, which has about 45 times higher concentration than the molarity of saturated vapour of XeF2 at 100 °C. Additionally, the high kinetic stability of XeF2 should be taken into consideration. For example, counterintuitively, XeF2 does not hydrolyse in aqueous solution instantaneously and it can be even extracted from aqueous solution by CCl₄ [24]. In CH₃CN solution XeF₂ is present in a non-ionized (molecular) form [20]. Higher fluorination activity can be achieved by addition of Lewis acids through formation of XeF⁺ and Xe₂F₃⁺ species [24]. A very effective fluorine atom source, the XeF• radical, would appear after the electron transfer to either of these cations. We did not add Lewis acids into reaction mixtures. However, transition metal ions demonstrate relatively strong Lewis acidity [28]. For example, it is not possible to prepare Ni2+ coordination compound with XeF2 molecule as a ligand, since the Lewis acidity of Ni²⁺ is sufficient to withdraw F⁻ ion from XeF₂ with Xe₂F₃⁺ formation [24]. Thus, our starting

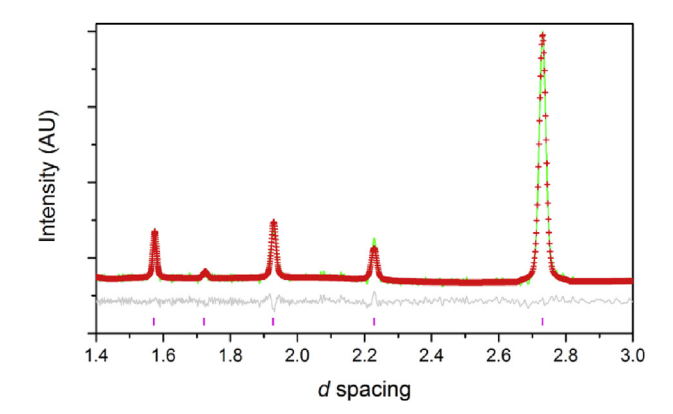


Fig. 1. Observed (crosses), calculated (green line), and difference (bottom grey line) profiles of Rietveld refinement of PXD data for $SrCoO_{2.5}F_{0.5}$ prepared by solvothermal fluorination at 100 °C. (For interpretation of the references to colour in this figure legend, the reader is referred to the Web version of this article.)

Table 1 Crystallographic data for $SrCoO_{2.5}F_{0.5}$ from Rietveld refinement of PXD data. ^a

Atomic position	Wyckoff position	х	у	z	10 ² Uiso (Å ²)	Occupancy
Sr1	1a	0	0	0	1.02 (3)	1
Co1	1b	0.5	0.5	0.5	0.54(2)	1
01	3c	0	0.5	0.5	1.32(5)	0.833
F1	3c	0	0.5	0.5	1.32(5)	0.167

 $[^]a$ Space group $\mbox{\it Pm}\overline{3}\mbox{\it m}$ (No. 221); a =3.8549 (1) Å; $R_{wp}=1.68\%;$ $R_p=1.58\%;$ and $\chi^2=0.961.$

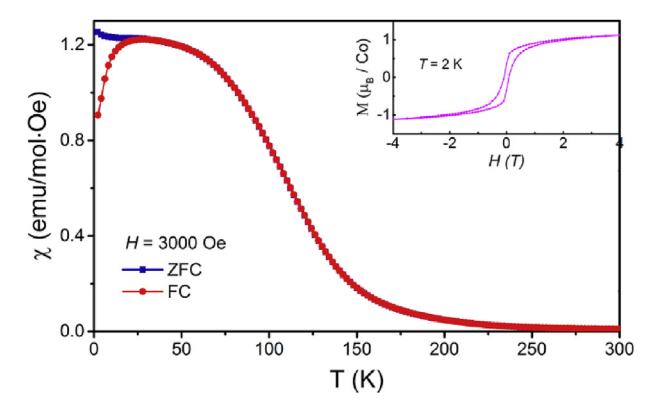


Fig. 2. Temperature dependence of DC magnetization for $SrCoO_{2.5}F_{0.5}$. Inset: magnetization vs. magnetic fields measurement at 2 K.

reagents, transition metal oxides with O vacancies, can activate XeF_2 . Additionally, it seems to be reasonable to assume that the presence of a solvent can lower the activation energy of a transition state for XeF_2 breakage. The stabilization can be expected since CH_3CN is a polar solvent, which are known to stabilize transition states for charged species in reactions. S_N1 type reactions are a typical example of the polar solvent effect. It is most probable that both factors: accessibility of higher XeF_2 concentrations and easier XeF_2 activation in the presence of the solvent – contribute to the efficiency of fluorination under solvothermal conditions at lower temperatures. Noteworthy, from the above consideration, it seems that pressure per se does not contribute to the method efficiency. However, higher pressure is clearly beneficial in the case of the solvothermal oxygen deintercalation method, since the reaction products have significantly smaller cell parameters [18].

While $SrCoO_{2.5}F_{0.5}$ can be prepared at $100~^{\circ}C$ by the solvothermal fluorination technique, we also tested the reaction at a higher temperature to understand the relative fluorinating power of this method. The reaction temperature was raised to $175~^{\circ}C$ ($50~^{\circ}C$ lower than the temperature used in the previous report of $SrCoO_{2.5}F_{0.5}$ preparation) [6]. The presence of $SrCoO_{2.5}F_{0.5}$ as well as substantial decomposition to the simple binary fluorides SrF_2 , and CoF_2 was observed after reacting for 24 h at $175~^{\circ}C$. The decomposition likely occurred due to over fluorination of the surface of grains, lending credence to the idea that solvothermal fluorination is more powerful than conventional solid-state fluorination methods.

3.2. Synthesis of $La_4Ni_3O_8F_1$ and $La_4Ni_3O_8F_2$ by solvothermal fluorination

In order to demonstrate a possibility of a broader utilization of the solvothermal fluorination method, attempts of synthesis of new oxyfluorides were undertaken. $Ni^{1+/2+}$ nickelate with NiO_2 infinite planes, $La_4Ni_3O_8$, was chosen as a starting compound for the fluorination. All known nickelates with infinite NiO_2 square-planar layers, are members of the T'-type $Ln_{n+1}Ni_nO_{2n+2}$ (Ln=La, Nd, Pr; n=2, 3, and ∞) homologous series [18,23,29–34]. Recently the T'-type nickelates received substantial

attention due to the discovery of superconductivity in thin-film of doped $n = \infty$ homologue (in $Nd_{0.8}Sr_{0.2}NiO_2$) [35].

It was shown earlier that the reduction of the parent Ruddlesden-Popper (RP) nickelate $La_4Ni_3O_{10}$ results in two distinct line phases: $La_4Ni_3O_9$ and $La_4Ni_3O_8$ [18]. The formation of the T'-type nickelate, $La_4Ni_3O_8$, from the RP phase occurs as a result of an oxygen deintercalation and a structural rearrangement in the $(LaO)_2$ part of the structure (Fig. 3). The oxygen atoms from the LaO layers in the perovskite blocks of the parent RP phases are completely removed during the reduction process. Additionally, rock-salt type $(LaO)_2$ block transforms to fluorite type arrangement by the shift of O atoms. This structural transformation is a mechanism of the internal structural stress release [23].

The reaction reversed to the RP phase reduction, oxidation of ${\rm La_4Ni_3O_8}$ with ${\rm La_4Ni_3O_{10}}$ formation, readily occurs above 175 °C in ${\rm O_2}$ flow (Fig. 3). Easy oxidation of ${\rm La_4Ni_3O_8}$ implies the possibility of fluorine intercalation instead of oxygen.

Initially, fluorination of La₄Ni₃O₈ by XeF₂ was tried without the addition of CH₃CN. The reaction of La₄Ni₃O₈ with XeF₂ at 350 °C (in a custom brass autoclave) led to the formation of LaOF and some amorphous products. Apparently, LaOF is the most thermodynamically stable phase in the La-Ni-O-F system and possible quaternary oxyfluorides are only kinetically stable and decompose to thermodynamically stable phases at higher temperatures. Nevertheless, a well-crystallized product was obtained by fluorination at 250 °C. This product was investigated by electron diffraction (ED) and energy dispersive X-ray (EDX) analysis. ED patterns taken from different crystallites can be separated into two groups according to distinct c/a ratio: ~7.0 for one phase and ~7.3 for the second one (Fig. 4). According to the EDX analysis both phases have the same La/Ni ratio but differ in F content with the estimated F content clearly higher for the phase with the larger c/a ratio. It can be concluded that a mixture of two new oxyfluorides, La₄Ni₃O₈F_x with different fluorine content was formed. Due to the close values of the X-ray form factors and the neutron scattering lengths for oxygen and fluorine, neither powder X-ray diffraction (PXD) nor powder neutron diffraction (PND) can generally be used for the determination of O/F ratios in oxyfluorides. However, both methods are reliable for establishing a total anion content. For oxyfluorides prepared by the reaction of La₄Ni₃O₈ with XeF₂ any total anion (O + F) content above eight can only be attributed to fluorine. The preliminary Rietveld refinement data of synchrotron powder X-ray diffraction data for the oxyfluoride with a lower fluorine content are provided in Supplementary Materials (Fig. S1, Table S1). The total anion content refined was 8.84, which leads to the stoichiometry of La₄Ni₃O₈F_{0.84}. A Le Bail fit for the oxyfluorides with the higher fluorine content was performed in Cmcm (63) space group (Fig. S2) deduced the

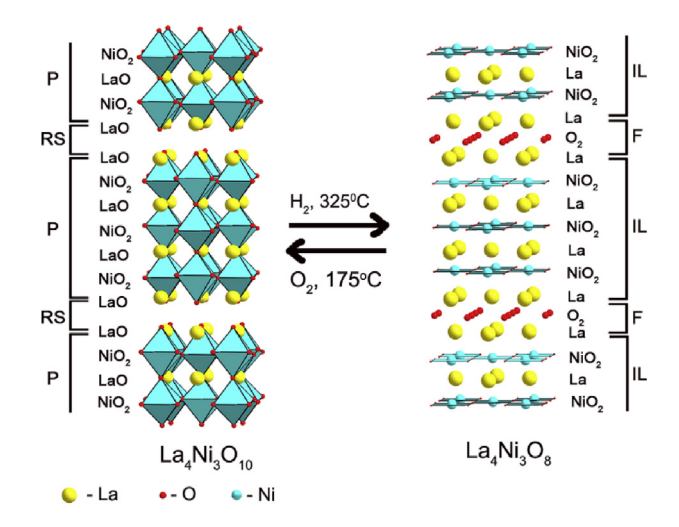


Fig. 3. Structure models of $La_4Ni_3O_{10}$ and $La_4Ni_3O_8$ with denoted layers and structural blocks: P, perovskite; RS, rock salt; IL, infinite layer; F, fluorite.

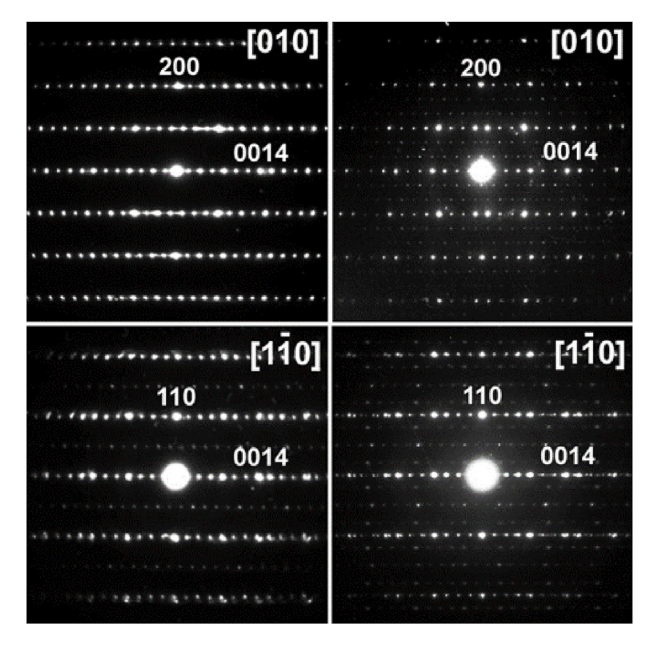


Fig. 4. Electron diffraction patterns of $La_4Ni_3O_8F_1$ (left column) and $La_4Ni_3O_8F_2$ (right column).

from electron diffraction experiments. A detailed structural study for the oxyfluorides will be reported separately. Ni K-edge X-ray absorption spectroscopy (XAS) measurements (Fig. S3) were used for estimation of the fluorine content in the fluorine rich oxyfluoride. By comparing with standards, nickel oxidation state close to 1.9 can be estimated, which results in the oxyfluorides stoichiometry of $\rm La_4Ni_3O_8F_x$ (x ~ 1.7). The oxyfluorides phases will be labelled $\rm La_4Ni_3O_8F_1$ and $\rm La_4Ni_3O_8F_2$ further in the text for convenience. The labels correspond to idealized stoichiometry and they are not meant to reflect the real fluorine content in the samples as some fluorine deficiency is definitely present in $\rm La_4Ni_3O_8F_1$ and most probably exist in $\rm La_4Ni_3O_8F_2$.

It was possible to optimize condition for solid-state synthesis of La₄Ni₃O₈F₁ phase at 250 °C. However, solid-state preparation of La₄Ni₃O₈F₂ required multiple intermediate grinding with the addition of a large XeF2 excess and resulted in broad peaks in the PXD patterns, probably due to F inhomogeneity. Therefore, the synthesis of La₄Ni₃O₈F₂ was undertaken by fluorination under solvothermal conditions. The relative ratio of $La_4Ni_3O_8$, $La_4Ni_3O_8F_1$, and $La_4Ni_3O_8F_2$ phases was monitored by comparing peak heights in the PXD patterns of the washed products after each reaction (Fig. 5). Initial attempts to produce $La_4Ni_3O_8F_2$ solvothermally at 50 °C and 75 °C proved unsuccessful after 10 days, resulting in pure starting material. As the reaction temperature was increased, La₄Ni₃O₈F₁ and La₄Ni₃O₈F₂ began to appear after 24 h at 100 °C and 150 °C; however, pure phase La₄Ni₃O₈F₂ was not isolated until a reaction temperature of 175 °C was used (Fig. 5). To check the method scalability, a large sample (~1 g) of La₄Ni₃O₈F₂ was successfully produced.

The syntheses of new oxyfluorides can be summarized by the following reaction schemes:

$$La_{4}Ni_{3}O_{10} \overset{H_{2},\ 325^{\circ}C}{\to} La_{4}Ni_{3}O_{8}\overset{XeF_{2},\ 250^{\circ}C}{\to} La_{4}Ni_{3}O_{8}F_{1} \tag{1}$$

$$La_4Ni_3O_{10} \stackrel{H_2, 325^{\circ}C}{\rightarrow} La_4Ni_3O_8 \stackrel{XeF_2, 175^{\circ}C (solvothermal)}{\rightarrow} La_4Ni_3O_8F_2$$
 (2)

For La₄Ni₃O₈F₁, which is an intermediate phase in the fluorination process, it was not possible to prepare single-phase sample without small amounts of either La₄Ni₃O₈, La₄Ni₃O₈F₂ or both admixture phases. Besides 2 admixture peaks denoted on Fig. 6, all other peaks can be indexed in tetragonal symmetry with a = 3.9314 (1) and c = 27.664 (1) Å (Fig. S1).

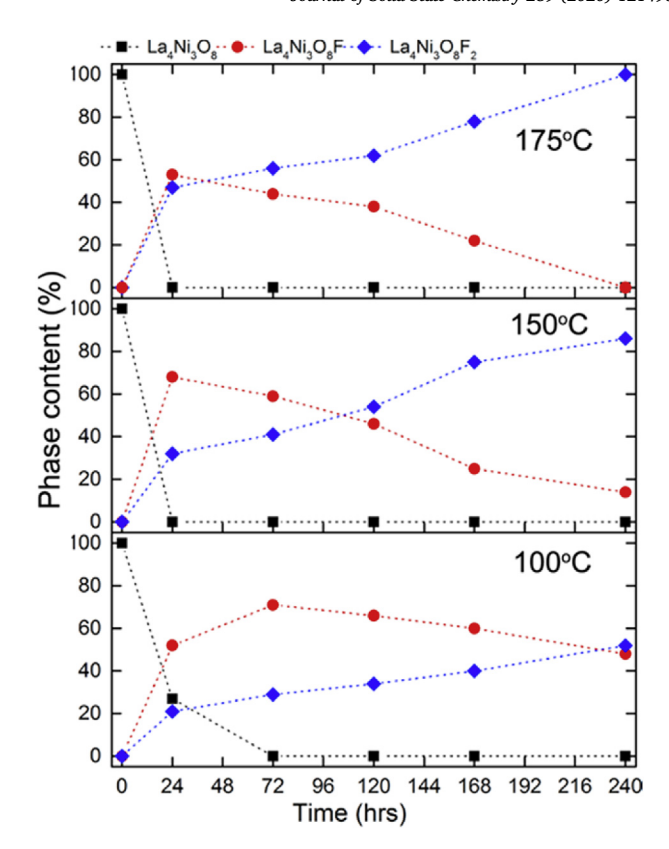


Fig. 5. Phase composition versus reaction time of La₄Ni₃O₈ solvothermal fluorination with XeF₂ in CH₃CN at 175 °C (top), 150 °C (middle), and 100 °C (bottom). La₄Ni₃O₈, black squares; La₄Ni₃O₈F₁, red circles; La₄Ni₃O₈F₂, blue rhombs. Relative phase content is normalized to 100% total. (For interpretation of the references to colour in this figure legend, the reader is referred to the Web version of this article.)

No peaks of impurity phases can be detected in the $\rm La_4Ni_3O_8F_2$ pattern. The peak indexing for data measured at 12 K (Fig. S2) was successful in orthorhombic symmetry with a=5.4390 (3), b=5.5210 (3) and c=29.804 (2) Å. Preliminary structural characterization indicate that crystal structure of $\rm La_4Ni_3^{2+}O_8F_2$ is similar to that of $\rm La_4Ni_3^{2.67+}O_{10}$. The unit cell parameters of $\rm La_4Ni_3^{20}O_{10}$ were reported to be a=5.415 (2), b=5.464 (2), c=27.96 (1) Å [23]. The c unit cell parameter of the oxyfluoride phase is 1.84 Å larger than that for the RP compounds. This large difference cannot be explained by difference in Ni oxidation states and it might indicate partial O/F ordering and the presence of highly elongated NiO₄F₂ octahedra in the structure. Detailed structural and density functional theory investigation of new oxyfluorides will be published separately.

Comparing temperatures of solvothermal fluorination needed for $SrCoO_{2.5}F_{0.5}$ and $La_4Ni_3O_8F_2$ preparation, one can notice that higher temperature was required in the latter case. Two factors contribute to the difference. While $SrCoO_{2.5}$ and $SrCoO_{2.5}F_{0.5}$ both crystallize in perovskite structures, substantial structural transformation is required during formation of $La_4Ni_3O_8F_2$ from $La_4Ni_3O_8$ (Fig. 3). The distance between Ni atoms from different layers in $La_4Ni_3O_8$ is only 3.26 Å, not sufficient for the formation of two Ni–F bonds after the F $^-$ insertion. Additionally, the $Ni^{1+/2+}$ Lewis acidity is much lower than that of Co^{3+} [28]. Per the discussion above, higher transition metal Lewis acidity facilitates XeF_2 activation.

Unlike to the previously reported in the literature solvothermal fluorination by XeF₂, where a complete anion exchange was observed with fluorides formation [16], the developed method utilizes a lower temperature range, which led to filling of anion vacancies in staring oxides with oxyfluorides formation. Thus, the method allows metastable

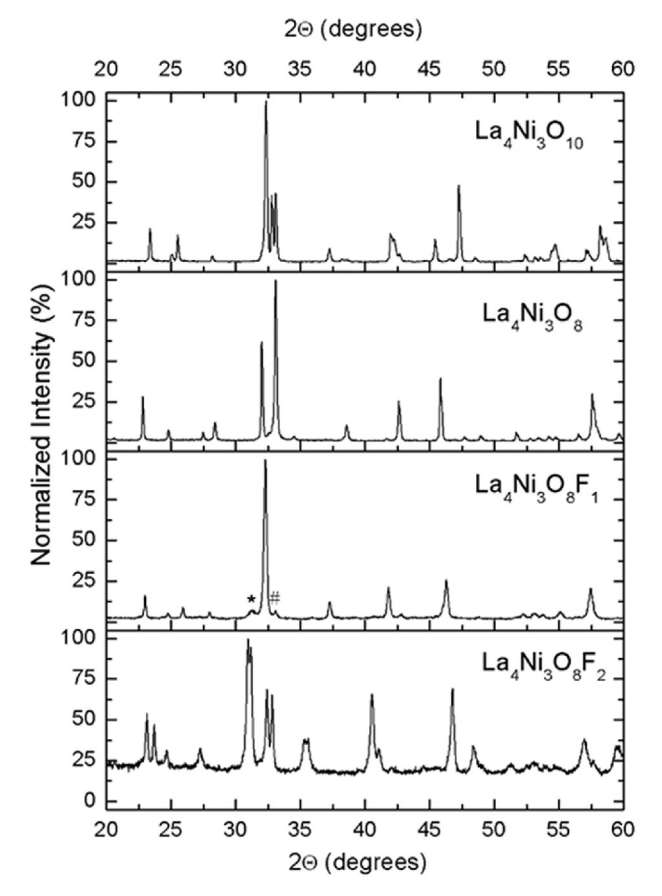


Fig. 6. Powder X-ray diffraction patterns for La $_4$ Ni $_3$ O $_{10}$, La $_4$ Ni $_3$ O $_8$, La $_4$ Ni $_3$ O $_8$ F $_1$ (solid-state synthesis) and La $_4$ Ni $_3$ O $_8$ F $_2$ (solvothermal preparation). * and # symbols denote peaks of La $_4$ Ni $_3$ O $_8$ F $_2$ and La $_4$ Ni $_3$ O $_8$ admixtures in the La $_4$ Ni $_3$ O $_8$ F $_1$ pattern.

oxyfluorides formation at lower temperatures, which contributes to soft chemistry reaction library of inorganic materials.

4. Conclusions

In conclusion, a facile low temperature solvothermal fluorination method is presented, which utilizes inexpensive commercial autoclaves and eliminate the need for intermediate grinding during fluorination. High solubility of XeF_2 in CH_3CN as well as the solvent polarity apparently facilitate the fluorination reaction at lower temperature. Most importantly, high fluorination activity at lower temperature provides access to metastable oxyfluorides inaccessible by other techniques; oxyfluorides decomposition is averted even for long (10 days) reaction time at optimized conditions. The improved control of fluorine diffusion allows for the careful design of new compounds with desired O/F ordering utilizing compounds with ordered oxygen vacancies as a structure directing templates. It can be expected that the method will become a standard fluorination technique in the solid-state chemistry synthetic method library.

Declaration of competing interest

The authors declare that they have no known competing financial interests or personal relationships that could have appeared to influence the work reported in this paper.

CRediT authorship contribution statement

Colin K. Blakely: Investigation, Visualization. Shaun R. Bruno:

Investigation. Shannon K. Kraemer: Investigation. Artem M. Abakumov: Investigation. Viktor V. Poltavets: Conceptualization, Writing - original draft, Writing - review & editing, Supervision, Project administration, Funding acquisition.

Acknowledgements

This work was supported by the National Science Foundation through grant DMR - 2004740.

Appendix A. Supplementary data

Supplementary data to this article can be found online at https://do i.org/10.1016/j.jssc.2020.121490.

References

- [1] C. Greaves, J.L. Kissick, M.G. Francesconi, L.D. Aikens, L.J. Gillie, Synthetic strategies for new inorganic oxide fluorides and oxide sulfates, J. Mater. Chem. 9 (1) (1999) 111–116.
- [2] E.E. McCabe, C. Greaves, Fluorine insertion reactions into pre-formed metal oxides, J. Fluor. Chem. 128 (4) (2007) 448–458.
- [3] H. Kageyama, K. Hayashi, K. Maeda, J.P. Attfield, Z. Hiroi, J.M. Rondinelli, K.R. Poeppelmeier, Expanding frontiers in materials chemistry and physics with multiple anions, Nat. Commun. 9 (2018).
- [4] B. Chevalier, A. Tressaud, B. Lepine, K. Amine, J.M. Dance, L. Lozano, E. Hickey, J. Etourneau, Stabilization of a new superconducting phase by low-temperature fluorination of La2cuo4, Physica C 167 (1–2) (1990) 97–101.
- [5] E.I. Ardashnikova, S.V. Lubarsky, D.I. Denisenko, R.V. Shpanchenko, E.V. Antipov, G. Vantendeloo, A new way of synthesis and characterization of superconducting oxyfluoride Sr2cu(O,F)(4+Delta), Physica C 253 (3-4) (1995) 259–265.
- [6] E. Sullivan, C. Greaves, Fluorine insertion reactions of the brownmillerite materials Sr2Fe2O5, Sr2CoFeO5, and Sr2Co2O5, Mater. Res. Bull. 47 (9) (2012) 2541–2546.
- [7] F.D. Romero, P.A. Bingham, S.D. Forder, M.A. Hayward, Topochemical fluorination of Sr-3(M0.5Ru0.5)(2)O-7 (M = Ti, Mn, Fe), n=2, ruddlesden-popper phases, Inorg. Chem. 52 (6) (2013) 3388–3398.
- [8] L.D. Aikens, R.K. Li, C. Greaves, The synthesis and structure of a new oxide fluoride, LaSrMnO4F, with staged fluorine insertion, Chem. Commun. 21 (2000) 2129–2130.
- [9] T. Sivakumar, J.B. Wiley, Topotactic route for new layered perovskite oxides containing fluorine: Ln(1.2)Sr(1.8)Mn(2)O(7)F(2) (Ln = Pr, Nd, Sm, Eu, and Gd), Mater. Res. Bull. 44 (1) (2009) 74–77.
- [10] P.R. Slater, Poly(vinylidene fluoride) as a reagent for the synthesis of K2NiF4related inorganic oxide fluorides, J. Fluor. Chem. 117 (1) (2002) 43–45.
- [11] M.G. Francesconi, P.R. Slater, J.P. Hodges, C. Greaves, P.P. Edwards, M. Al-Mamouri, M. Slaski, Superconducting Sr(2-x)A(x)CuO(2)F(2+delta) (A = Ca, Ba): synthetic pathways and associated structural rearrangements, J. Solid State Chem. 135 (1) (1998) 17–27.
- [12] C.K. Blakely, J.D. Davis, S.R. Bruno, S.K. Kraemer, M.Z. Zhu, X.L. Ke, W.L. Bi, E.E. Alp, V.V. Poltavets, Multistep synthesis of the SrFeO2F perovskite oxyfluoride via the SrFeO2 infinite-layer intermediate, J. Fluor. Chem. 159 (2014) 8–14.
- [13] A.M. Abakumov, M.G. Rozova, E.I. Ardashnikova, E.V. Antipov, High-temperature superconductors based on complex layered copper oxyfluorides, Russ. Chem. Rev. 71 (5) (2002) 383–399.
- [14] T. Katayama, A. Chikamatsu, Y. Hirose, R. Takagi, H. Kamisaka, T. Fukumura, T. Hasegawa, Topotactic fluorination of strontium iron oxide thin films using polyvinylidene fluoride, J. Mater. Chem. C 2 (27) (2014) 5350–5356.
- [15] F. Schreine, G.N. Mcdonald, C.L. Chernick, Vapor pressure and melting points of xenon difluoride and xenon tetrafluoride, J Phys Chem-Us 72 (4) (1968) 1162–1166
- [16] G.R. Waetzig, G.A. Horrocks, J.W. Jude, L. Zuin, S. Banerjee, X-ray excited photoluminescence near the giant resonance in solid-solution Gd1-xTbxOCl nanocrystals and their retention upon solvothermal topotactic transformation to Gd1-xTbxF3, Nanoscale 8 (2) (2016) 979–986.
- [17] R. Pandey, A.B. Kunz, Characterization of fluorine-doped magnesium-oxide a computer-simulation study, J. Phys. Chem. Solid. 51 (8) (1990) 929–931.
- [18] C.K. Blakely, S.R. Bruno, V.V. Poltavets, Low-temperature solvothermal approach to the synthesis of La4Ni3O8 by topotactic oxygen deintercalation, Inorg. Chem. 50 (14) (2011) 6696–6700.
- [19] W.W. Dukat, J.H. Holloway, E.G. Hope, P.J. Townson, R.L. Powell, The reactions of xenon difluoride with inert solvents, J. Fluor. Chem. 62 (2–3) (1993) 293–296.
- [20] H. Meinert, S. Rudiger, Zur chemie der edelgasverbindungen das system xenondifluorid/acetonitril, Z. Chem. 7 (6) (1967) 239.
- [21] J. Sheng, K.B. Tang, Z.H. Liang, Y.K. Wang, D. Wang, W.Q. Zhang, Solvothermal fluorination: a new chemical fluorination method to insert fluorine into Sr2CuO3 and NdSr2Cu2O6-delta, Mater. Chem. Phys. 115 (1) (2009) 483–487.
- [22] E. Sullivan, J. Hadermann, C. Greaves, Crystallographic and magnetic characterisation of the brownmillerite Sr2Co2O5, J. Solid State Chem. 184 (3) (2011) 649–654.
- [23] V.V. Poltavets, K.A. Lokshin, M. Croft, T.K. Mandal, T. Egami, M. Greenblatt, Crystal structures of Ln(4)Ni(3)O(8) (Ln = La, Nd) triple layer T '-type nickelates, Inorg. Chem. 46 (25) (2007) 10887–10891.

- [24] M. Tramsek, B. Zemva, Synthesis, properties and chemistry of xenon(II) fluoride, Acta Chim. Slov. 53 (2) (2006) 105–116.
- [25] H.M. Rietveld, A profile refinement method for nuclear and magnetic structures, J. Appl. Crystallogr. 2 (1969) 65–&.
- [26] A.C. Larson, R.B. Von Dreele, Los Alamos National Laboratory Report LAUR, vol. 86, Los Alamos National Laboratory: Los Alamos, NM, 2000, p. 748.
- [27] B.H. Toby, EXPGUI, a graphical user interface for GSAS, J. Appl. Crystallogr. 34 (2001) 210–213.
- [28] Y.G. Zhang, Electronegativities of elements in valence states and their applications .2. A scale for strengths of Lewis-acids, Inorg. Chem. 21 (11) (1982) 3889–3893.
- [29] N. ApRoberts-Warren, J. Crocker, A.P. Dioguardi, K.R. Shirer, V.V. Poltavets, M. Greenblatt, P. Klavins, N.J. Curro, NMR evidence for spin fluctuations in the bilayer nickelate La3Ni2O6, Phys. Rev. B 88 (7) (2013), 075124.
- [30] N. ApRoberts-Warren, A.P. Dioguardi, V.V. Poltavets, M. Greenblatt, P. Klavins, N.J. Curro, Critical spin dynamics in the antiferromagnet La4Ni3O8 from La-139 nuclear magnetic resonance, Phys. Rev. B 83 (1) (2011).
- [31] O.O. Bernal, D.E. MacLaughlin, G.D. Morris, P.C. Ho, L. Shu, C. Tan, J. Zhang, Z. Ding, K. Huang, V.V. Poltavets, Charge-stripe order, antiferromagnetism, and

- spin dynamics in the cuprate-analog nickelate La4Ni3O8, Phys. Rev. B 100 (12) (2019)
- [32] V.V. Poltavets, M. Greenblatt, G.H. Fecher, C. Felser, Electronic properties, band structure, and fermi surface instabilities of Ni1+/Ni2+ nickelate La3Ni2O6, isoelectronic with superconducting cuprates, Phys. Rev. Lett. 102 (4) (2009).
- [33] V.V. Poltavets, K.A. Lokshin, S. Dikmen, M. Croft, T. Egami, M. Greenblatt, La3Ni2O6: a new double T '-type nickelate with infinite Ni1+/2+O2 layers, J. Am. Chem. Soc. 128 (28) (2006) 9050–9051.
- [34] V.V. Poltavets, K.A. Lokshin, A.H. Nevidomskyy, M. Croft, T.A. Tyson, J. Hadermann, G. Van Tendeloo, T. Egami, G. Kotliar, N. ApRoberts-Warren, A.P. Dioguardi, N.J. Curro, M. Greenblatt, Bulk magnetic order in a twodimensional Ni1+/Ni2+ (d(9)/d(8)) nickelate, isoelectronic with superconducting cuprates, Phys. Rev. Lett. 104 (20) (2010).
- [35] D.F. Li, K. Lee, B.Y. Wang, M. Osada, S. Crossley, H.R. Lee, Y. Cui, Y. Hikita, H.Y. Hwang, Superconductivity in an infinite-layer nickelate, Nature 572 (7771) (2019), 624-+.